Biogeochemistry (2023) 164:207–228
https://doi.org/10.1007/s10533-022-00945-5

Isotopic evidence for sources of dissolved carbon and the role of organic matter respiration in the Fraser River basin, Canada

Britta M. Voss · Timothy I. Eglinton · Bernhard Peucker-Ehrenbrink · Valier Galy · Susan Q. Lang · Cameron McIntyre · Robert G. M. Spencer · Ekaterina Bulygina · Zhaohui Aleck Wang · Katherine A. Guay

Received: 20 December 2021 / Accepted: 23 May 2022 / Published online: 10 July 2022
© The Author(s) 2022

Abstract Sources of dissolved and particulate carbon to the Fraser River system vary significantly in space and time. Tributaries in the northern interior of the basin consistently deliver higher concentrations of dissolved organic carbon (DOC) to the main stem than other tributaries. Based on samples collected near the Fraser River mouth throughout 2013, the radiocarbon age of DOC exported from the Fraser River does not change significantly across seasons despite a spike in DOC concentration during the freshet, suggesting modulation of heterogeneous upstream chemical and isotopic signals during transit through the river basin. Dissolved inorganic carbon (DIC) concentrations are highest in the Rocky Mountain headwater region where carbonate weathering is evident, but also in tributaries with high DOC concentrations, suggesting that DOC respiration may be responsible for a significant portion of DIC in this basin. Using an isotope and major ion mass balance

Responsible Editor: Penny Johnes.

Supplementary Information The online version contains supplementary material available at https://doi.org/10.1007/s10533-022-00945-5.

B. M. Voss (✉) · B. Peucker-Ehrenbrink · V. Galy · Z. A. Wang · K. A. Guay
Woods Hole Oceanographic Institution, 360 Woods Hole Road, Falmouth, MA 02543, USA
e-mail: brittamv@gmail.com

B. M. Voss
Massachusetts Institute of Technology, 77 Massachusetts Avenue, Cambridge, MA 02139, USA

Present Address:
B. M. Voss
Department of Ecology, 300 Desmond Dr, Lacey, WA 98503, USA

T. I. Eglinton · C. McIntyre
Eidgenössische Technische Hochschule, Sonneggstrasse 5, 8092 Zürich, Switzerland

B. Peucker-Ehrenbrink
University of the Fraser Valley, 33844 King Road, Abbotsford, BC V2S 7M7, Canada

S. Q. Lang
University of South Carolina, 701 Sumter St, Columbia, SC 29208, USA

Present Address:
C. McIntyre
Scottish Universities Environmental Research Centre, Glasgow G750QF, UK

R. G. M. Spencer
Florida State University, 600 West College Avenue, Tallahassee, FL 32306, USA

R. G. M. Spencer · E. Bulygina
Woodwell Climate Research Center, 149 Woods Hole Road, Falmouth, MA 02540, USA

Present Address:
E. Bulygina
Old Dominion University Research Foundation, 4600 Elkhorn Ave, Norfolk, VA 23529, USA

approach to constrain the contributions of carbonate and silicate weathering and DOC respiration, we estimate that up to 33 ± 11% of DIC is derived from DOC respiration in some parts of the Fraser River basin. Overall, these results indicate close coupling between the cycling of DOC and DIC, and that carbon is actively processed and transformed during transport through the river network.

Keywords River · Carbon isotopes · Radiocarbon · Weathering · Carbon cycle

Introduction

Rivers convey large quantities of dissolved organic carbon (DOC) and dissolved inorganic carbon (DIC) from terrestrial environments to the coastal ocean, with the global export flux of DOC from rivers (~0.25 Gt C a^{-1}; Hedges et al. 1997; Cai 2011) sufficient to compensate for the estimated annual loss of global marine DOC (Eglinton and Repeta 2014). DOC carried by rivers undergoes rapid biological and abiotic processing within terrestrial watersheds, with the majority subject to remineralization before it reaches the ocean (Catalán et al. 2016). The typically supersaturated state of dissolved CO_2 in rivers is at least partially a consequence of microbial and photochemical conversion of OC to CO_2, and results in significant outgassing of CO_2 from river surfaces (Cole and Caraco 2001; Butman and Raymond 2011; Raymond et al. 2013; Reiman and Xu 2018). Consequently, lateral fluxes of dissolved carbon are less than would occur if rivers functioned as simple pipes, transferring terrestrial material to the ocean (Raymond et al. 2013; Butman et al. 2016; Schädel et al. 2016).

Quantifying the extent of in-transit degradation of riverine organic matter is critical to assessing the role of watersheds in the consumption versus release of atmospheric CO_2 (Perdue et al. 1976; Cole and Caraco 2001; Battin et al. 2009; Tranvik et al. 2009; Aufdenkampe et al. 2011). However, constraining DOC transport and transformation of riverine organic matter is challenging due to seasonal changes in temperature, hydrology, and biology, which affect both the amount and type of material mobilized in river channels over the course of a year, as well as its turnover and transformation along the aquatic continuum. Furthermore, different portions of river basins—potentially draining watersheds containing different vegetation types, soil characteristics, and bedrock lithologies—may produce DOC and DIC in varying quantities and with different organic matter (OM) composition and lability. In situ primary and secondary productivity within rivers represent additional sources (and sinks) of DOC and DIC. Identifying geochemical indicators of riverine OC provenance and lability may help elucidate the links between watershed characteristics and ecological behavior, and aid in extending conclusions drawn from process studies of CO_2 efflux rates on small spatial scales to larger watersheds.

The present study aims to link spatial and temporal variations in the isotopic characteristics of DOC and DIC on the scale of a river basin in order to develop a holistic perspective of source materials and processes of OM alteration during riverine transport. We focus on dissolved as opposed to particulate carbon phases, because of the ~3 × greater flux of the former (Voss et al. 2015), while acknowledging the potential for interaction and exchange between phases. The study area, the Fraser River basin in southwestern Canada (Fig. 1), provides a unique setting for such a study due to two main features: (*i*) its modest size (~232,000 km^2) and accessibility allows for a detailed characterization of the majority of its tributary basins, while (*ii*) its variety of bedrock lithology (including carbonate outcrops in certain tributary basins) and spatial and temporal precipitation gradients impart naturally large variability in biogeoclimatic zones, and water geochemistry (Voss et al. 2014), and thus, potentially, gradients in carbon isotopes.

Previous work on the impact of bedrock diversity and seasonal hydrology on dissolved and particulate inorganic constituents in the Fraser basin (Cameron et al. 1995; Cameron 1996; Cameron and Hattori 1997; Voss et al. 2014, 2015) has documented the importance of detailed basin-wide characterizations of source compositions and seasonal sampling to understand the provenance and variability of material reaching the river mouth in this heterogeneous system. This study now extends this approach to basin-scale carbon dynamics. The use of bulk

Present Address:
K. A. Guay
Bowdoin College, 6800 College Station, Brunswick, ME 04011, USA

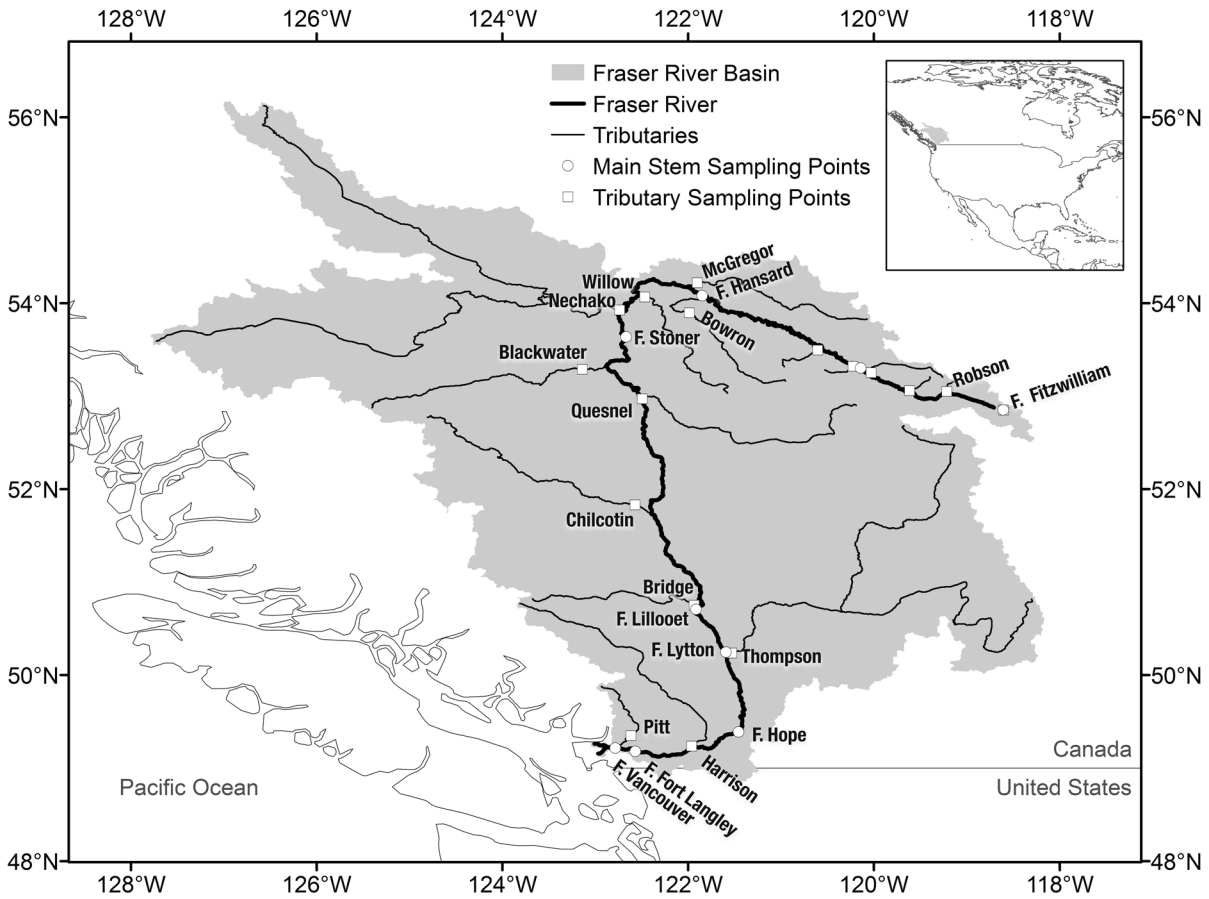

Fig. 1 Map of the Fraser River Basin and major tributaries sampled in this study. Inset map indicates the location of the Fraser River Basin in North America. "F" before a station name indicates locations on the Fraser main stem. Time series samples were collected at the Fraser at Fort Langley station (Table 2)

concentrations and isotope compositions allows for the quantification of the relative influence of chemical weathering and biological processing on the geochemical composition of dissolved carbon pools exported by the Fraser River.

Methods

DIC and DOC concentrations

Samples for DIC were collected and analyzed following well-established procedures (e.g. Wang et al. 2016; Song et al. 2020). Briefly, samples were collected by pumping water in-line over membrane filters (0.45 µm pore size used for 2009 and 2010 samples; 0.2 µm pore size for 2011 samples) into pre-cleaned (with mild Liquinox soap solution and rinsed thoroughly with purified water) 250 mL borosilicate glass bottles with ground glass stoppers. Bottles were overfilled with 3×the sample volume and poisoned immediately with 60 µL saturated $HgCl_2$ solution. Glass stoppers were sealed with vacuum grease (Apiezon M) and secured with rubber bands. DIC samples preserved in this way are very stable. For example, one sample from this study (Fraser River at Vancouver sampled in July 2009) was analyzed at 12 and 21 months after collection, and the measured DIC concentrations were within 3%. Nearly all samples were analyzed within one year of collection; however, two samples (Thompson River and Bridge River sampled in July 2009) were analyzed 1.7 and 2.5 years after collection, respectively.

DIC concentration was measured on a DIC analyzer (Apollo SciTech LLC., Model AS-C3) at Woods Hole Oceanographic Institution (WHOI). The measurements are based on acidification of water samples (by 10% H_3PO_4), followed by N_2 gas stripping of CO_2 in the acidified samples and infrared detection of CO_2 by a LiCOR® 7000 CO_2 analyzer (Wang et al. 2017). The DIC analyzer was calibrated by Certified Reference Materials of DIC provided by Dr. A.G. Dickson at the Scripps Institution of Oceanography (Dickson 2010; Sarma et al. 2011).

Samples for DOC concentration measurements were filtered in the same manner as DIC samples and collected in 20–60 mL low-density polyethylene bottles (precleaned with 10% HCl). Although the filter pore size differed between some of the sampling campaigns, previous studies have found such differences to have a minimal effect on measured DOC concentration and composition (Nimptsch et al. 2014; Spencer 2022, pers. comm.). Samples were acidified with 12 N HCl to pH 2 in the field and stored refrigerated until analysis. DOC concentrations were analyzed by high temperature combustion on a Shimadzu TOC analyzer within 1–3 months after sample collection. Based on a series of duplicate measurements (n = 20 pairs), precision is better than 10% for samples with DOC concentration > 200 µmol L^{-1} and better than 20% for samples > 100 µmol L^{-1}.

^{13}C and ^{14}C analyses of DOC and DIC

Samples for DOC and DIC isotope analyses were filtered in the same manner as those for concentration analyses but collected in different bottles. DOC isotope samples were collected in pre-combusted (450 °C, 5 h) 1 L amber glass bottles and acidified immediately with H_3PO_4 (Certified ACS grade) to pH 2. DIC isotope samples were collected in combusted (450 °C, 5 h) 500 mL borosilicate glass bottles, poisoned immediately with 100 µL of saturated $HgCl_2$ solution, and sealed with greased (Apiezon M) ground glass stoppers and rubber bands. DIC isotope samples were analyzed at the National Ocean Science Accelerator Mass Spectrometry (NOSAMS) facility in Woods Hole, USA, and DOC isotope samples were analyzed at either NOSAMS or the Laboratory for Ion Beam Physics at the Eidgenössische Technische Hochschule (ETH) in Zürich, Switzerland.

DOC isotope samples were analyzed by either UV oxidation (Beaupré et al. 2007) or by wet chemical oxidation, a method which has been shown to be comparable to UV oxidation (Lang et al. 2016). Briefly, for UV oxidation, DOC samples were sparged to remove DIC, then UV-irradiated for 4 h and sparged on an in-line vacuum line cryo-trap; evolved CO_2 was converted to graphite and analyzed for ^{14}C by accelerator mass spectrometry (AMS) at NOSAMS (Roberts et al. 2010); a split of CO_2 was collected for ^{13}C analysis by dual-inlet isotope ratio MS (IRMS) (McNichol et al. 2000). For wet chemical oxidation, samples were sparged in Exetainer vials containing potassium persulfate, then heated to 100 °C to allow quantitative conversion of DOC to CO_2; evolved CO_2 was directly sampled from vials and injected onto a gas ion source AMS at ETH for ^{14}C analysis (see Lang et al. 2016, for detailed methodology). DOC isotope measurements were performed between 1 and 2 years after sample collection.

DIC samples were sparged, CO_2 converted to graphite following collection of a CO_2 split for ^{13}C analysis by IRMS, and analyzed for ^{14}C by AMS at NOSAMS. DIC isotope measurements were performed 9 months after sample collection. Combined sampling and absolute analytical precision for $\delta^{13}C$ data generated with these methods has been previously reported as 0.03–0.05‰ (McNichol et al. 2000). NOSAMS DOC results have been revised based on the recent procedural blank correction assessment (Xu et al. 2021). Absolute analytical precision for NOSAMS $\Delta^{14}C$-DOC was better than 54‰, and for ETH $\Delta^{14}C$-DOC was better than 40‰. Absolute analytical precision for NOSAMS $\Delta^{14}C$-DIC was better than 4‰.

Results

Dissolved organic and inorganic carbon distribution of the Fraser River

The dissolved carbon budget of the Fraser River is dominated by DIC. At nearly every site and all times of year, the concentration of DIC is the largest component of total dissolved carbon species (DIC + DOC), constituting 80% on average (Table 1, Fig. 2A–C). Relatively high concentrations of DIC are found in particular tributaries (Robson,

Table 1 Dissolved carbon data

Site	Date (yyyy-mm-dd)	DIC (µmol L^{-1})	DOC (µmol L^{-1})	DIC Flux (mol s^{-1})	DOC Flux (mol s^{-1})	δ^{13}C-DIC		δ^{13}C-DOC		Δ^{14}C-DIC		Δ^{14}C-DOC	
						(‰)	Lab ID	(‰)	Lab ID	(‰)	Lab ID	(‰)	Lab ID
Fraser at Fitzwilliam	2010-10-14	803	117	29	4.2								
Fraser at Fitzwilliam	2009-08-03	506	44	43	3.8	− 4.28	OS-79353	− 25.85	OS-147290	− 110.4	OS-79353	46.4	OS-147290
Fraser at Fitzwilliam	2011-06-03	719	189	77	20.2								
Fraser at McBride	2010-10-14	1106	69	164	10.2								
Fraser at McBride	2009-08-04	708	20	321	9.3			− 26.15	OS-147302			− 19.8	OS-147302
Fraser at McBride	2011-06-02	891	161	421	76.3								
Fraser at Hansard	2010-10-16	2012	297	537	79.3								
Fraser at Hansard	2009-08-04	1103	54	767	37.4								
Fraser at Hansard	2011-06-01	1065	233	1513	331.5								
Fraser at Stoner	2010-10-19		243										
Fraser at Stoner	2009-08-08	981	199			− 6.73	OS-79356	− 24.92	OS-147296	− 145.5	OS-79356	94.0	OS-147296
Fraser at Lillooet	2010-10-21		235		214.7								
Fraser at Lillooet	2009-08-10		156		329.9	− 6.40	OS-79360	− 26.61	OS-147294	− 141.5	OS-79360	84.6	OS-147294
Fraser at Lillooet	2011-05-28	1077	642	6636	3957.1			− 27.49	OS-149273			47.3	OS-149273
Fraser at Lytton	2010-10-22		205										
Fraser at Lytton	2009-08-01	953	145										

Table 1 (continued)

Site	Date (yyyy-mm-dd)	DIC (µmol L^{-1})	DOC (µmol L^{-1})	DIC Flux (mol s^{-1})	DOC Flux (mol s^{-1})	δ^{13}C-DIC		δ^{13}C-DOC		Δ^{14}C-DIC		Δ^{14}C-DOC	
						(‰)	Lab ID	(‰)	Lab ID	(‰)	Lab ID	(‰)	Lab ID
Fraser at Hope	2010-10-24		216		406.4								
Fraser at Hope	2011-05-27	797	418	7004	3674.8								
Fraser at Fort Langley	2010-10-25	1015	193	2222	423.0								
Fraser at Fort Langley	2009-07-30	824		3870		− 6.26	OS-79351			− 118.7	OS-79351		
Fraser at Fort Langley	2009-08-13	798	131	2725	448.5			− 26.58	OS-147297			71.7	OS-147297
Fraser at Fort Langley	2011-06-07	893	386	9039	3903.6								
Fraser at Van-couver shallow	2009-07-28	660	130	3018	594.5	− 6.49	OS-79349	− 26.72	OS-147288	− 124.7	OS-79349	59.4	OS-147288
Fraser at Vancou-ver deep	2009-07-28	672	132	3072	601.3	− 6.62	OS-79350			− 129.1	OS-79350		
Robson River	2010-10-14	1416	31										
Robson River	2009-08-03	1211	17			− 4.57	OS-79354	− 25.74	OS-147300	− 294.3	OS-79354	66.7	OS-147300
Robson River	2011-06-03	1594	62										
Bowron River	2009-08-05	1561	108	39	2.7								
Bowron River	2011-05-31	1083	365	328	110.7								
McGregor River	2010-10-16	1671	177	204	21.6								

Table 1 (continued)

Site	Date (yyyy-mm-dd)	DIC (µmol L^{-1})	DOC (µmol L^{-1})	DIC Flux (mol s^{-1})	DOC Flux (mol s^{-1})	δ^{13}C-DIC		δ^{13}C-DOC		Δ^{14}C-DIC		Δ^{14}C-DOC	
						(‰)	Lab ID	(‰)	Lab ID	(‰)	Lab ID	(‰)	Lab ID
McGregor River	2009-08-05	1366	27	287	5.7			− 26.68	OS-147301			− 39.6	OS-147301
McGregor River	2011-06-01	1126	211	772	145.1								
Willow River	2010-10-15	1042	289	11	3.1								
Willow River	2009-08-06	1185	276	9	2.1								
Willow River	2011-05-31	536	694	124	160.4								
Nechako River	2010-10-17	1124	437	120	46.8								
Nechako River	2009-08-06	737	395	417	223.8	− 6.38	OS-79355	− 27.24	OS-147291	− 3.8	OS-79355	95.6	OS-147291
Nechako River	2011-05-31	868	850	650	635.9								
Stuart Lake	2009-08-07	885	488	215	118.6								
Blackwater River	2010-10-18	1553	466	38	11.3								
Blackwater River	2009-08-08	1631	546	36	12.2	− 8.74	OS-79357	− 26.36	OS-147292	− 56.4	OS-79357	74.1	OS-147292
Blackwater River	2011-05-30	986	1479	410	615.2			− 27.12	OS-149272			74.3	OS-149272
Quesnel River	2010-10-19	1061	124	134	15.7								
Quesnel River	2009-08-09	983	88	271	24.3	− 4.73	OS-79358	− 26.22	OS-147298	− 135.4	OS-79358	69.6	OS-147298
Quesnel River	2011-05-30	1125	268	931	221.7								
Chilcotin River	2010-10-20	733	90	72	8.8								
Chilcotin River	2009-08-09	518	83	130	20.9	− 3.80	OS-79359	− 25.92	OS-147299	− 26.1	OS-79359	44.7	OS-147299

Table 1 (continued)

Site	Date (yyyy-mm-dd)	DIC (µmol L^{-1})	DOC (µmol L^{-1})	DIC Flux (mol s^{-1})	DOC Flux (mol s^{-1})	δ^{13}C-DIC		δ^{13}C-DOC		Δ^{14}C-DIC		Δ^{14}C-DOC	
						(‰)	Lab ID	(‰)	Lab ID	(‰)	Lab ID	(‰)	Lab ID
Chilcotin River	2011-05-29	1396	1055	302	227.9			− 27.05	OS-149271			70.2	OS-149271
Bridge River	2010-10-21	1684	70										
Bridge River	2009-08-10		49										
Bridge River	2011-05-28		205										
Thompson River	2010-10-22	733	172	315	73.8								
Thompson River	2009-08-01	598	115	578	111.6	− 5.36	OS-79352	− 26.44	OS-147289	− 71.5	OS-79352	70.0	OS-147289
Thompson River	2011-05-27	812	414	1915	976.8								
Harrison River	2010-10-24	397	127	114	36.4								
Harrison River	2009-07-31	295	74	197	49.5			− 26.19	OS-147295			39.6	OS-147295
Harrison River	2011-05-26	343	115	196	65.6								
Pitt River	2010-10-25		118										
Pitt River	2011-05-26	140	139										

All dissolved organic and inorganic carbon data. Lab ID indicates NOSAMS accession numbers. See Supplementary Information (Table S2) for sample locations and discharge information

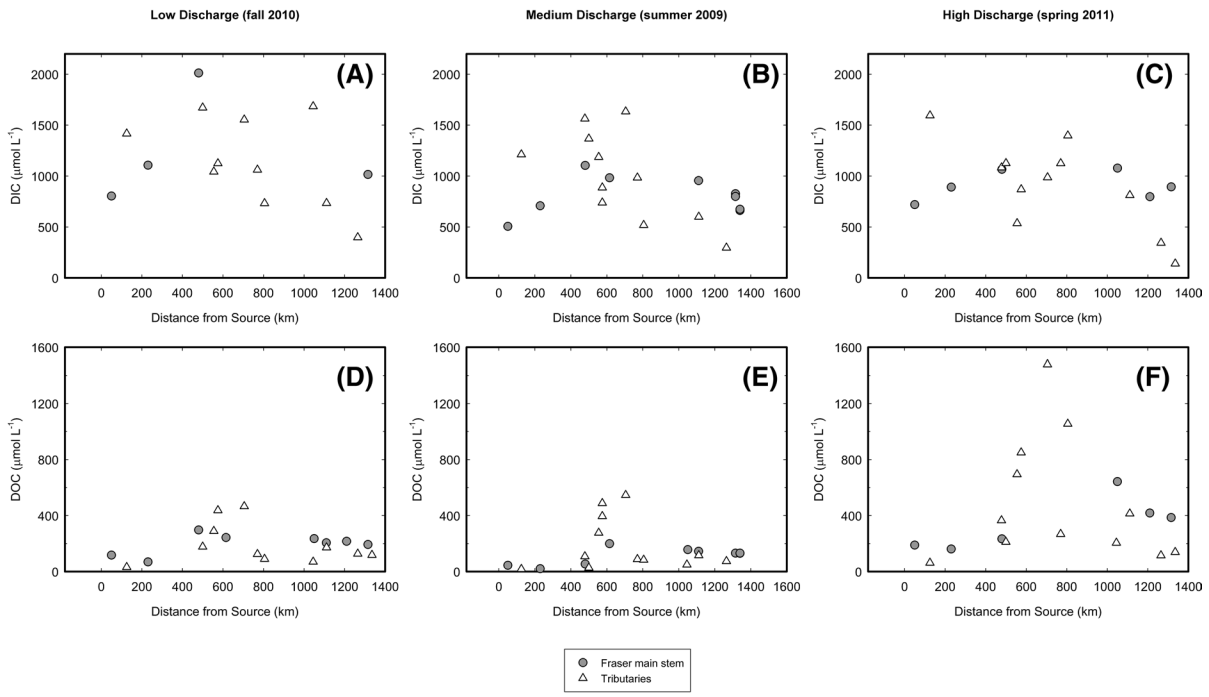

Fig. 2 Concentrations (µmol L^{-1}) of DIC (panels A-C) and DOC (panels D-F) across the Fraser basin at low discharge (left panels), medium discharge (center panels), and high discharge (right panels)

McGregor, Blackwater, Willow, and Bridge rivers), which span a wide swath of the Fraser basin and are not restricted to areas draining particular bedrock lithologies (Wheeler et al. 1991). Tributaries with relatively low DIC concentrations (Harrison and Pitt rivers), however, represent areas dominated by acidic intrusive igneous rocks and minor metamorphic units of the Coast Belt with presumably only finely disseminated carbonate minerals, but no carbonate-rich sedimentary lithologies. DOC exhibits a very different spatial pattern (Fig. 2D–F), with the highest concentrations in tributaries draining the peneplain region upstream of Prince George (Nechako and Willow rivers), and a Coast Range tributary, the Blackwater River, with especially high DOC concentrations (466–1479 µmol L^{-1}) relative to all other sites under all flow conditions. Another group of tributaries (the Bridge, McGregor, Robson, Pitt, and Harrison rivers) is notable for its relatively low DOC concentration (< 212 µmol L^{-1}).

DIC and DOC fluxes are generally highest under high discharge conditions and lowest during low discharge conditions across tributaries of the Fraser River (Fig. 3). The Thompson River, which contributes the greatest proportion (~20–25%) of discharge to the Fraser River of all tributaries, also accounts for the largest proportions of DOC and DIC fluxes under nearly all discharge conditions. The only exception is that, under medium discharge conditions, the Nechako River DOC flux was the greatest of all tributaries, on account of the relatively high DOC concentrations in the northern peneplain portion of the basin. The eight tributaries shown in Fig. 3 account for 45–61% of the DIC flux, and 51–82% of the DOC flux, of the Fraser River at Fort Langley near the coast under the three observed flow conditions.

Isotopic signatures of DOC and DIC

The isotope compositions of Fraser basin tributaries and points along the main stem were measured primarily in samples collected during medium discharge conditions in summer 2009 (Fig. 4). The stable carbon isotopic composition of DIC (δ^{13}C-DIC) ranged from − 8.7 to − 3.8‰, with the highest values occurring in tributaries of the central portion of the basin (Quesnel, Chilcotin, and Thompson rivers) and the headwaters (Fraser River at Fitzwilliam and Robson

Table 2 DOC time series

DOC concentrations, fluxes and $\Delta^{14}C$ values throughout 2013 near the mouth of the Fraser River (at Fort Langley). Samples with the same date are lab splits for the ^{14}C analysis. Lab ID indicates ETH sample numbers

Date (yyyy-mm-dd)	DOC (μmol L^{-1})	DOC Flux (mol C s^{-1})	$\Delta^{14}C$ (‰)	Absolute $\Delta^{14}C$ error (‰)	Lab ID
2013-01-12	257	273	− 65.0	21.9	56,995.1.1
2013-02-09	248	248	− 26.1	23.7	56,997.1.1
2013-02-09	248	248	1.5	28.8	56,998.1.1
2013-03-16	242	349	− 49.9	23.8	56,999.1.1
2013-03-30	205	270	− 9.9	29.5	56,987.1.1
2013-03-30	205	270	31.5	35.3	56,988.1.1
2013-04-07	266	608	2.8	22.1	56,989.1.1
2013-04-10	415	1132	24.1	17.5	56,991.1.1
2013-04-16	558	1599	24.8	13.3	56,993.1.1
2013-05-01	760	3480	− 29.5	10.5	57,001.1.1
2013-05-17	389	4322	28.9	17.3	57,003.1.1
2013-06-22	226	1938	5.0	26.5	57,005.1.1
2013-07-24	184	840	14.2	31.1	57,007.1.1
2013-07-24	184	840	− 25.7	31.6	57,008.1.1
2013-09-20	130	319	− 2.7	38.3	57,009.1.1
2013-10-25			− 106.1	30.6	57,011.1.1
2013-11-15			21.1	34.8	57,013.1.1
2013-12-19			− 68.7	31.4	57,015.1.1

River). Corresponding $\delta^{13}C$-DOC values spanned a narrower range, from − 27.5 to − 24.9‰. Inter-sample variability in $\delta^{13}C$-DOC samples was small relative to data precision, therefore further interpretation of these data is not warranted.

The $\Delta^{14}C$-DIC values of main stem sites are relatively invariant across the basin, ranging from − 110 to − 145‰. In contrast, tributaries of the central portion of the basin (Nechako, Blackwater, Quesnel, Chilcotin, and Thompson rivers) are more variable, with relatively high $\Delta^{14}C$-DIC (− 135 to − 4‰; younger ^{14}C age) compared to a lower $\Delta^{14}C$-DIC value (older ^{14}C age) for the sole site analyzed in the Rocky Mountains (Robson River, − 294‰). The $\Delta^{14}C$-DOC values of most sites in the Fraser basin are higher than those of DIC, corresponding to near

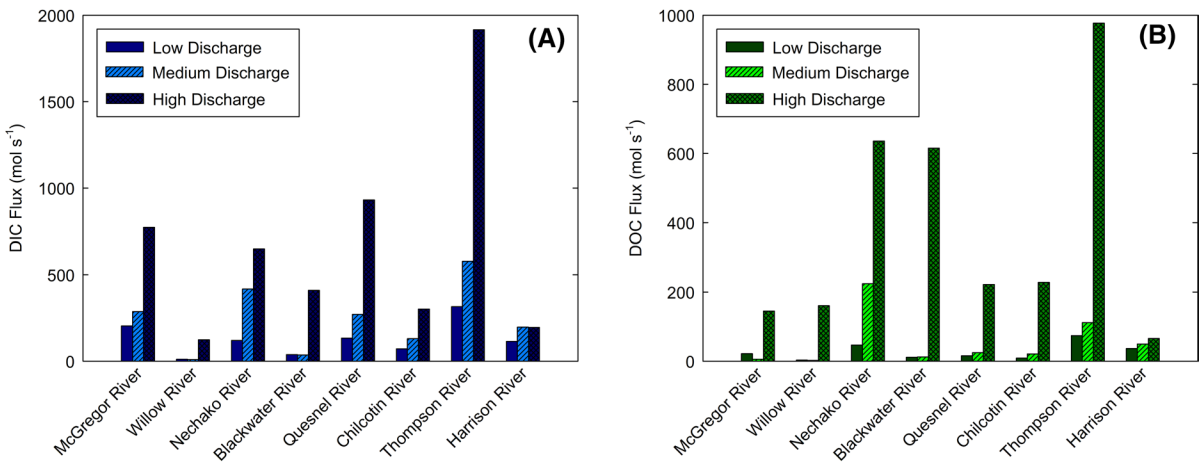

Fig. 3 DIC (A) and DOC (B) fluxes (mol s^{-1}) in tributaries of the Fraser River under low, medium, and high discharge conditions. Note the difference in scale of the axes

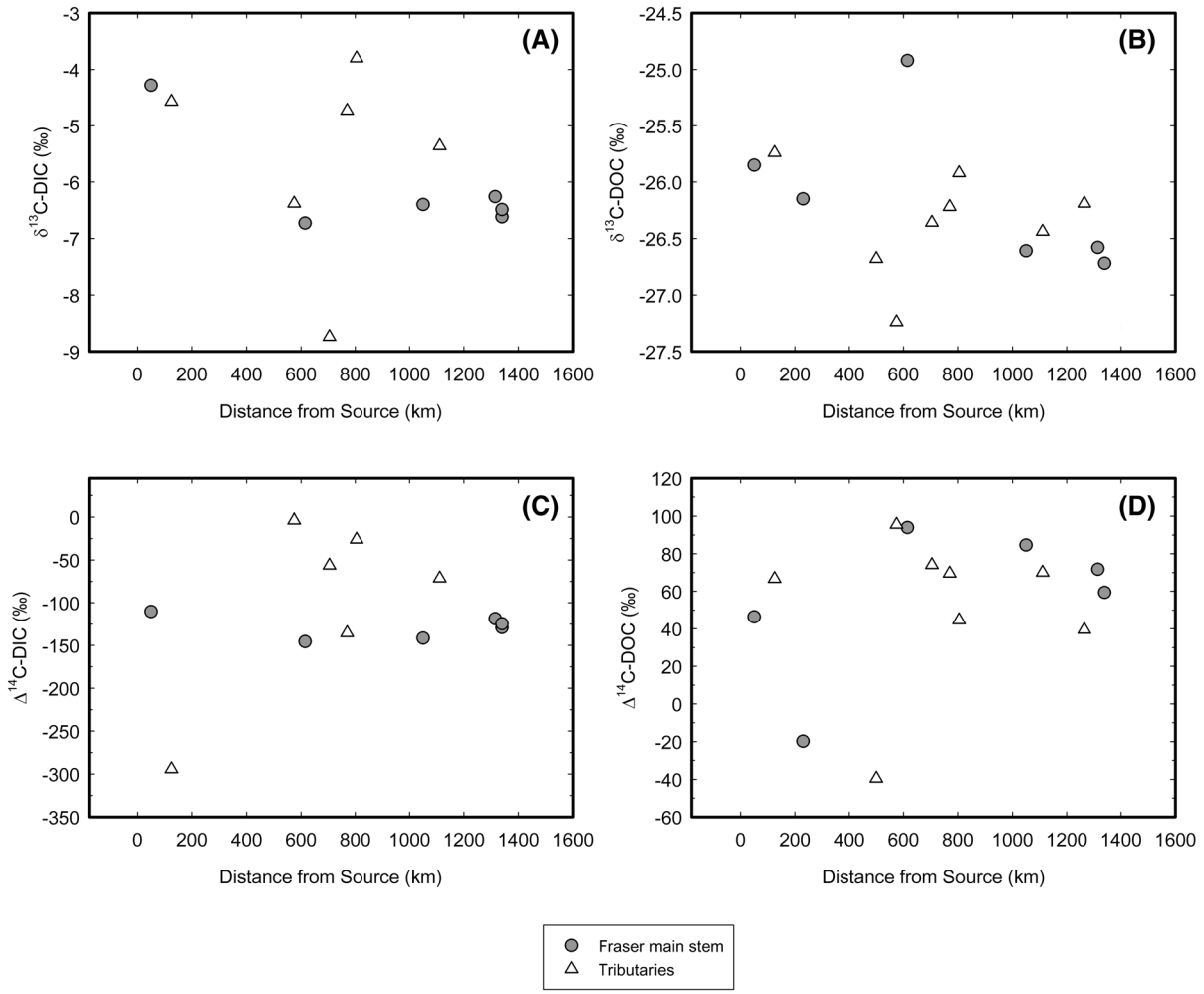

Fig. 4 Isotope compositions (‰) of Fraser basin dissolved carbon pools in summer 2009: $\delta^{13}C$ of DIC (A) and DOC (B) and $\Delta^{14}C$ of DIC (C) and DOC (D). Note that precision for $\delta^{13}C$ data is approximately 0.03–0.05‰ (McNichol et al. 2000), which is minor compared to inter-sample variability for $\delta^{13}C$-DIC data, but significant for $\delta^{13}C$-DOC data

modern or greater-than-modern (i.e., post-bomb) ^{14}C ages. Three sites (Fraser River at Lillooet and Blackwater and Chilcotin rivers) from the high discharge period in 2011 were also analyzed for $\delta^{13}C$ and $\Delta^{14}C$ values of DOC. In the case of $\delta^{13}C$-DOC, the values for these sites during high discharge were 0.8–1.1‰ lower than those during medium discharge, while there were no consistent differences between high and medium discharge for $\Delta^{14}C$-DOC values. The $\Delta^{14}C$-DOC value in the Fraser River at Lillooet was 37‰ higher during medium discharge than during high discharge, whereas the $\Delta^{14}C$-DOC value in the Blackwater River was nearly identical in medium and high discharge samples and the Chilcotin River was 25‰ lower during medium discharge than during high discharge.

In 2013, $\Delta^{14}C$-DOC samples collected near the mouth of the Fraser River over the course of a full year (Fig. 5A) ranged from − 106 to + 31‰, with a mean of − 13 ± 39‰ (1 s.d.). The average measurement uncertainty was ± 26‰ (representing the 1σ measurement error propagated through the correction for the presence of the processing blank). DOC did not exhibit any clear temporal trends in $\Delta^{14}C$ values.

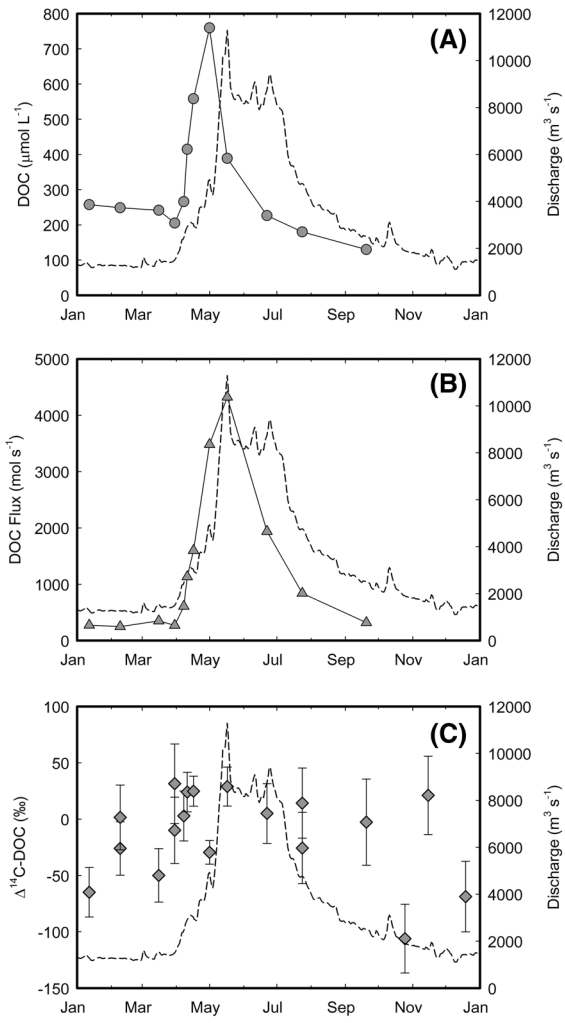

Fig. 5 The 2013 time series record of (A) DOC concentration and (B) DOC flux exhibit a pronounced pulse in the early stages of the spring freshet followed by a rapid decay. In contrast, the Δ^{14}C-DOC during this period (C) is relatively constant and nearly modern throughout the year. Fraser River discharge is shown on each panel as a dashed line

Discussion

Flow-dependence and spatial patterns of DOC and DIC

Concentrations of DIC and DOC in the Fraser River main stem exhibit similar downstream trends. In general, concentrations are relatively low in the Rocky Mountain headwaters, elevated in the central portion of the basin, and gradually decline for roughly the second half of the river's length. The tributary inputs of each of these pools, however, are distinct, contributing to spatial variability and varying in their response to seasonal changes in discharge.

The downstream pattern of tributary DOC concentrations features relatively low concentrations in tributaries draining the Rocky Mountains and the lower Coast Range, and higher concentrations in tributaries draining the central portion of the basin (Cariboo and upper Coast Range). This pattern likely reflects the thin and immature soils in the mountainous headwaters in contrast with the more established soils and low-lying wetland areas of the central and lower portion of the basin. The main stem Fraser exhibits a similar spatial pattern, with rising DOC concentrations from the headwaters until Hansard/Stoner (~500 km from the river source), followed by a slight decrease as the river enters the relatively arid central basin, which continues for the remainder of its course.

While this spatial pattern is consistent between the different flow regimes, the absolute concentrations vary substantially. DOC concentrations are lowest in the samples collected during medium discharge (summer), somewhat higher during low discharge (fall), and highest during the spring freshet. This freshet DOC pulse is a common feature of many high-latitude rivers (Holmes et al. 2008; Cooper et al. 2008; Guo et al. 2012), and results from changing hydrologic flowpaths as surface soils across the basin become inundated (to an average depth of 0.2–0.8 m), releasing DOM accumulated throughout the previous fall and winter (Voss et al. 2015). In the Fraser basin, with the wide variety of biogeoclimatic zones and land cover (Valentine et al. 1978), the initiation of the spring freshet can vary by a few weeks between individual tributary basins. Therefore, the high discharge samples from spring 2011 likely capture slightly different stages of the freshet DOC pulse in each tributary sub-basin.

The seasonal variations in DIC concentrations are notably decoupled from those of DOC, suggesting the influence of additional drivers (other than DOC remineralization). DIC is the single largest component of the dissolved load of the Fraser River and its concentration at most sites varies only modestly between high, medium, and low discharge conditions, suggesting DIC fluxes are primarily driven by the amount of discharge (Table 3). In contrast, the variability in DOC concentrations across different discharge

Table 3 DIC time series

Date (yyyy-mm-dd)	DIC (μmol L^{-1})	DIC Flux (mol C s^{-1})
2009-07-30	824	3870
2009-08-13	798	2725
2010-10-25	1015	2222
2011-05-25	913	7841
2011-06-07	893	9351
2011-06-26	800	7886
2011-06-28	794	7955
2011-07-08	770	7458
2011-07-15	877	8553
2011-07-19	839	8098
2011-10-14	782	2124
2011-10-25	892	2012
2011-10-26	864	1931
2011-10-31	900	1940
2011-11-15	1011	1972
2011-12-12	1003	1281
2012-01-11	937	1646
2012-02-10	1073	1300
2012-07-05	798	8308
2012-07-13	765	7425

DIC concentrations and fluxes near the mouth of the Fraser River (at Fort Langley)

conditions supports the assertion that the sources of DOC change in nature throughout the year (Voss et al. 2015).

Sources of DOC

The relatively ^{14}C-depleted values of DOC in headwater areas of the Fraser basin indicate the mobilization of aged organic material, which may derive from soil, bedrock, and/or anthropogenic sources (i.e., products of fossil fuel utilization). Combustion-derived aerosols are a significant source of ancient OC in surface waters and soils globally (Jaffé et al. 2013). In the lower Fraser River downstream of the major tributaries, black carbon, with a $\Delta^{14}C$ value of ~ − 570‰, constitutes 6.9 ± 0.5% of the POC pool (Coppola et al. 2018), and on a global basis dissolved black carbon is estimated to account for ~ 10% of the global riverine flux of DOC (Jaffé et al. 2013). DOC in streams draining coastal and mountainous glaciers of western North America in particular have been shown to contain a significant aged component, most likely from aerosols derived from fossil fuel combustion (Hood et al. 2009; Stubbins et al. 2012), and there is evidence of combustion-derived OM in the Fraser basin dating back to the early Holocene (Hallett et al. 2003). Though less directly impacted by air masses originating from east Asia (the predominant source for aerosols to the North American west coast), some fossil fuel combustion-derived aerosols may be deposited on mountain glaciers of the Fraser basin. However, if this is the case, it is not clear why relatively old DOC would be restricted only to these headwater basins, given that most major tributaries of the Fraser River have headwaters fed by glaciers (Thorne and Woo 2011). It may be that glacial-derived DOC is relatively bio-labile and is rapidly degraded, as has been observed in other streams and rivers (Hood et al. 2009; Hemingway et al. 2019), leaving little ^{14}C evidence in downstream DOC samples. The importance of glacial influence may be obscured by differences in residence time between tributaries given that the tributaries carrying relatively aged DOC are smaller than most of the others analyzed. It is currently not possible to exclude contributions of fossil combustion residues to the ^{14}C-depleted DOC signals given current uncertainties concerning the reactivity of dissolved combustion-derived components (Stubbins et al. 2012; Wagner et al. 2021), but the lack of coherence in values across tributaries suggests that aged DOC in the Fraser system is driven by processes other than deposition of anthropogenic combustion-derived aerosols on glaciers. Instead, we speculate that ^{14}C-depleted DOC in the Fraser River and its tributaries is primarily derived from mobilization and dissolution of pyrogenic fossil carbon and pre-aged biogenic OM in soils and glacial debris. Further information on DOM composition and dynamics is needed to fully address the question of DOC provenance in the Fraser basin.

As a test of the above hypothesis that DOC respiration is an important source of DIC in the Fraser River, it might be expected that DIC $\delta^{13}C$ values would reflect isotopic signatures associated with DOC consumption. DIC derived from respiration of C_3 plant material (with a $\delta^{13}C$ value of ~ − 27‰) would be expected to have a $\delta^{13}C$ value of ~ − 18‰ (Clark and Fritz 1997), while DIC derived from weathering of carbonate or silicate rocks would be expected to have $\delta^{13}C$ values of approximately − 8.25‰ and − 17‰,

respectively (Spence and Telmer 2005). In situ primary production may also influence $\delta^{13}C$ values, resulting in a residual DIC pool with higher $\delta^{13}C$ values. The $\delta^{13}C$ values of DIC (− 3.8 to − 8.7‰) and DOC (− 24.9 to − 27.5‰) in the Fraser River likely reflect the interplay of leaching and respiration of C_3 plant material and mineral weathering and possibly aquatic autotrophic biomass (although the Fraser basin is on the whole heterotrophic; Raymond et al. 2013). The data from this study cannot fully disentangle the impact of these sources on bulk DIC and DOC $\delta^{13}C$ values. Future studies which specifically investigate the magnitude and spatial and temporal variation of autotrophic production in the Fraser River and the distribution of carbonate-bearing soils would shed light on the relative importance of these sources as an independent comparison with the contribution of respired DOC to the DIC pool estimated here.

Weathering and respiration controls on load and composition of DIC and DOC

The inorganic geochemical composition of dissolved material provides multiple indicators of the influence of carbonate weathering in certain portions of the Fraser basin (Voss et al. 2014). The relatively high DIC concentrations in certain tributaries also suggest a contribution from carbonate-rich lithologies; however, other weathering reactions also produce DIC (Blattmann et al. 2019; Hilton and West 2020), while biological consumption or production of DIC may also affect riverine DIC loads (Voss et al. 2017). The dissolved inorganic load of the Fraser River (excluding carbonate species) is essentially a binary mixture of carbonate- and silicate-derived weathering products (Voss et al. 2014), although sulfide weathering also occurs in certain regions (Cameron et al. 1995; Spence and Telmer 2005). The major cation composition (Ca/Na and Mg/Na) of the Robson River in particular resembles that of runoff from carbonate-dominated lithologies (Meybeck 1986; Gaillardet et al. 1999), and therefore its composition likely reflects major element contributions due almost entirely to carbonate weathering. Sites in other parts of the basin, however, reflect a more complex combination of biogeochemical processes impacting the dissolved load.

To quantify the importance of carbonate weathering, silicate weathering, and OM respiration to the DIC load of the Fraser, we used the concentrations of dissolved major elements, DIC, and DOC, and corresponding carbon isotopic compositions, in a series of mass balance relationships. Dissolved major element data for these samples were previously reported by Voss et al. (2014). We applied these calculations to the eight sites from the medium discharge sampling campaign in 2009 for which we have complete concentration and isotopic composition data (i.e., the main stem Fraser River at Fitzwilliam, Stoner, and Vancouver shallow; and tributaries Nechako, Blackwater, Quesnel, Chilcotin, and Thompson rivers). First, carbonate- and non-carbonate-derived DIC fractions are constrained by their ^{13}C and ^{14}C values:

$$f_{carb} + f_{NC} = 1 \tag{1}$$

$$f_{carb}\delta_{carb} + f_{NC}\delta_{NC} = \delta_{meas} \tag{2}$$

$$f_{carb}\Delta_{carb} + f_{NC}\Delta_{NC} = \Delta_{meas} \tag{3}$$

where δ and Δ represent the stable and radiocarbon isotope compositions, respectively, of DIC from carbonate weathering (*carb*), non-carbonate-weathering processes (*NC*), and measured samples (*meas*). The proportions of carbonate-weathering-derived DIC (f_{carb}) and non-carbonate-weathering-derived DIC (f_{NC}) can be approximated from dissolved major ion composition, after correction for sea salt aerosols. As dissolved chloride is almost entirely derived from sea salt aerosols in the Fraser River (Voss et al. 2014), we correct other major ion concentrations as follows:

$$[X]_{nss} = [X]_{meas} - [Cl]_{meas}\left(\frac{X}{Cl}\right)_{ss} \tag{4}$$

where X is any major ion, *nss* indicates non-sea-salt-derived, and *ss* is sea-salt-derived. The Robson River, with major ion ratios very similar to a pure carbonate weathering endmember (Gaillardet et al. 1999), is used to estimate the non-carbonate-weathering-derived fraction of DIC in other sites as follows:

$$f_{NC} = \frac{[DIC]_{NC}}{[DIC]_{meas}} = \frac{1}{[DIC]_{meas}}\left[DIC_{meas} - \left(\frac{Ca+Mg}{Na}\right)_{nss} \times \left(\frac{DIC}{(Ca+Mg)/Na}\right)_{Robson}\right] \tag{5}$$

The sea salt aerosol correction is complicated for the Robson River medium discharge sample as the dissolved Cl value of 43 µmol L^{-1} reported by Voss et al. (2014) is very high compared to corresponding values at low and high discharge (4.6 and 5.7 µmol L^{-1}, respectively), suggesting that it is likely influenced by sources other than atmospheric aerosols. Given that this sample has a Na concentration of 9.5 µmol L^{-1} (Voss et al. 2014), if this sample contained Na exclusively from sea salt aerosols, it would be expected to have a Cl concentration of only 11 µmol L^{-1} (based on a sea salt Na/Cl composition of 0.86). As silicate weathering must also contribute some Na to the dissolved load, such an elevated Cl concentration cannot represent natural processes. Furthermore, Cl concentrations for other Rocky Mountain tributaries, i.e. McGregor, Holmes, and Small rivers, under all discharge conditions range from 1.9 to 5.5 µmol L^{-1}, and all other Fraser basin samples under medium discharge conditions do not exceed 18.5 µmol L^{-1} (Voss et al. 2014). We therefore chose to correct the sea salt contribution to the medium discharge Robson River sample using a Cl concentration of 3 µmol L^{-1}, which represents the lower range of Cl concentrations for Rocky Mountain tributaries during this sampling time, and therefore yields a lower-limit estimate of non-carbonate DIC in other Fraser basin samples. The choice of Cl concentration estimate for this sample is clearly important; however, within reasonable bounds, the exact value does not substantially alter the result and interpretation of the estimate of non-carbonate DIC. The quantitative impact of the choice of this value is evaluated later in this section.

The isotope composition of DIC derived from carbonate weathering contains signatures from both carbonic acid weathering and sulfuric acid weathering of carbonate minerals. The impact of sulfuric acid weathering can be estimated with a similar mass balance:

$$f_C + f_S = 1 \tag{6}$$

$$f_C\delta_C + f_S\delta_S = \delta_{carb} \tag{7}$$

$$f_C\Delta_C + f_S\Delta_S = \Delta_{carb} \tag{8}$$

where C and S indicate carbonic acid weathering of carbonates and sulfuric acid weathering of carbonates, respectively. Since carbonic acid weathering of carbonates produces one mole of carbon derived from soil CO_2 (a mixture of atmospheric CO_2 and soil organic matter respiration) and one mole from the carbonate mineral being dissolved, δ_C is the average of the $\delta^{13}C$ composition of soil CO_2 adjusted for the fractionation effect of dissolution (predominantly as HCO_3^- at typical Fraser River pH), or ~ − 17‰, and mineral $CaCO_3$, ~ 0.5‰, i.e., ~ − 8.25‰ (Spence and Telmer 2005). Likewise, Δ_C is the average $\Delta^{14}C$ of modern atmospheric CO_2 at the time of sampling (~ 48‰; Graven et al. 2012) and mineral $CaCO_3$ (−1000‰, assuming any secondary soil carbonate is negligible), or ~ − 476‰. Sulfuric acid weathering of carbonates produces DIC derived only from mineral $CaCO_3$, therefore δ_S = ~ 0.5‰ (Spence and Telmer 2005) and Δ_S = − 1000‰.

In principle, the sulfuric acid contribution to carbonate weathering (f_S) can be approximated based on patterns of SO_4^{2-} concentrations and stable sulfur isotope values of sulfate. Practically, however, this requires careful consideration of a range of endmembers (e.g., evaporites, atmospheric deposition) as well as potential alterations of the values via microbial sulfate reduction along the course of the river (e.g., Calmels et al. 2007; Torres et al. 2016; Hemingway et al. 2020). Yet, the low SO_4^{2-} concentrations and high values in the Fraser basin reported in the literature (Cameron et al. 1995; Spence and Telmer 2005; Voss et al. 2014; Burke et al. 2018) allow for rough constraints on the relative contribution of sulfuric acid to carbonate weathering. Spence and Telmer (2005) estimated DIC fluxes for carbonate weathering by carbonic acid and carbonate weathering by sulfuric acid for a range of sites across the basin, demonstrating that sulfuric acid-based carbonate weathering is 1–30% of the total carbonate weathering DIC flux at most sites (with the exception of the headwaters of the Lillooet River, which drains an area with active hydrothermal activity and unaccounted-for cation fluxes). The sulfuric acid contribution to DIC fluxes reported for the main stem and the largest tributary (Thompson River) are 5% and 8%, respectively, while higher sulfuric acid weathering contributions (Chilcotin and Cayoosh rivers) are associated with Coast Range tributaries which also likely capture hydrothermically active areas. Therefore, we assert that the average f_S value of the Fraser basin lies in the range of 5–10%, and we estimate f_S is ~ 0.08. We

further note that the exact value of f_S within reasonable bounds does not significantly impact our isotope mass balance, as will be described later. Using these values, we solve Eqs. 6–8 for f_C, δ_{carb}, and Δ_{carb}, and subsequently Eqs. 1–3 can be solved for δ_{NC} and Δ_{NC}.

Next, we construct a mass balance for non-carbonate-weathering-derived DIC, which is derived from silicate weathering, OM respiration, and atmospheric CO_2 invasion:

$$f_{SWOM} + f_{atm} = 1 \tag{9}$$

$$f_{SWOM}\delta_{SWOM} + f_{atm}\delta_{atm} = \delta_{NC} \tag{10}$$

$$f_{SWOM}\Delta_{SWOM} + f_{atm}\Delta_{atm} = \Delta_{NC} \tag{11}$$

where *atm* refers to atmospheric CO_2 and *SWOM* to the combination of organic matter respiration and silicate weathering. We group OM respiration and silicate weathering together because the isotopic signatures of DIC produced by each of these processes are practically indistinguishable, and the DIC contribution from silicate weathering is quantified separately below. The values of δ_{SWOM} and δ_{atm} are estimated as the measured $\delta^{13}C$ values of DOC (as an approximation of soil CO_2 composition) and modern atmospheric CO_2, respectively, both adjusted for a ~ 9.6‰ fractionation effect due to speciation from $CO_2(g)$ to $HCO_3^-(aq)$, which assumes all DIC is HCO_3^-, and an average Fraser River water temperature of 10 °C. Similarly, the values of Δ_{SWOM} and Δ_{atm} are estimated as the measured $\Delta^{14}C$ values of DOC and modern atmospheric CO_2, respectively. Based on these values, Eqs. 9–11 can be solved for f_{SWOM} and f_{atm}.

Next, we construct a mass balance for DIC, composed of contributions from carbonate weathering, atmospheric CO_2 invasion, and OM respiration + silicate weathering:

$$f_{carb} + f_{atm}f_{NC} + f_{SWOM}f_{NC} = 1 \tag{12}$$

$$[DIC] = f_{carb}[DIC] + f_{atm}f_{NC}[DIC] + f_{SWOM}f_{NC}[DIC] \tag{13}$$

and a second mass balance to isolate the silicate-weathering-derived portion of f_{SWOM}:

$$f_{SWOM}f_{NC}[DIC] = [DIC]_{sil} + [DIC]_{DOC} = [DIC]\left(f_{sil} + f_{DOC}\right) \tag{14}$$

where f_{sil} is the portion of DIC produced by silicate weathering and f_{DOC} is the portion produced by OM respiration, which is assumed to be entirely derived from DOC, either in soil pore waters, groundwater, or in the river. By doing so, we implicitly neglect contributions from respiration of old soil organic carbon and weathering of petrogenic carbon. The former is consistent with observations that soil organic carbon respiration is dominated by young organic carbon from the soil organic horizon (Trumbore 2000). The latter is likely reasonable considering the low petrogenic C concentrations in most bedrocks in the Fraser River catchment as well as in Fraser River suspended sediments (Voss et al. 2014; Galy et al. 2015). The silicate weathering contribution can be estimated based on the major ion composition of each site in comparison to carbonate and silicate end-members as follows:

$$f_{sil} = \frac{(Ca/Na)_{meas} - (Ca/Na)_{carb}}{(Ca/Na)_{sil} - (Ca/Na)_{carb}} \tag{15}$$

where $(Ca/Na)_{carb}$ and $(Ca/Na)_{sil}$ represent the molar Ca/Na composition of carbonate and silicate weathering end-members. Long-term observations of molar Mg/Na vs. Ca/Na in the main stem Fraser River (e.g. Voss et al. 2014) exhibit a correlation of approximately (Mg/Na) = 0.21*(Ca/Na) + 0.42 (n = 111, $r^2 = 0.93$). We therefore applied a silicate end-member composition of 0.2, which is at the low end of the range defined by Gaillardet et al. (1999), and used this value to solve the above correlation for Mg/Na, yielding a value of 0.46. For the carbonate end-member, we used the Robson River composition (Ca/Na = 75, rather than 50 as suggested by Gaillardet et al. 1999) to better match the lithology of the Fraser basin. These values are also comparable to carbonate and silicate weathering Ca/Na end-member compositions reported by Négrel et al. (1993) of 60 ± 30 and 0.35 ± 0.25, respectively. The silicate- and non-silicate-weathering-derived portions of each major element can then be calculated as follows, applying Ca/Na (as defined above) and HCO_3/Na end-member compositions from Gaillardet et al. (1999):

$$[Na]_{sil} = f_{sil}[Na]_{nss} \tag{16}$$

$$[Na]_{non-sil} = [Na]_{nss} - [Na]_{sil} \tag{17}$$

Table 4 Estimates of DIC derived from DOC respiration

Site	$[DIC]_{DOC}$ (µmol L^{-1})	f_{DOC}
Fraser at Fitzwilliam	3	0.01
Fraser at Stoner	326	0.33
Fraser at Vancouver shallow	108	0.16
Nechako River	142	0.19
Blackwater River	434	0.27
Quesnel River	209	0.21
Chilcotin River	23	0.04
Thompson River	96	0.16

The portion of DIC derived from DOC respiration, expressed as a concentration ($[DIC]_{DOC}$) and as a fraction of total DIC (f_{DOC}), demonstrates that DOC respiration can constitute a significant portion of the total DIC load

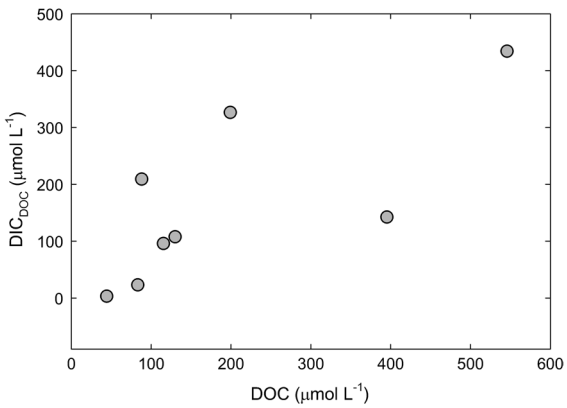

Fig. 6 The correlation between the estimated contribution of DOC respiration to the DIC load (DIC_{DOC}; $r^2 = 0.53$) supports the isotope mass balance approach to this calculation

$$[Ca]_{non-sil} = [Na]_{non-sil} \times \left(\frac{Ca}{Na}\right)_{carb} \quad (18)$$

$$[Ca]_{sil} = [Ca]_{nss} - [Ca]_{non-sil} \quad (19)$$

$$\left[HCO_3\right]_{sil} = [Na]_{sil} \times \left(\frac{HCO_3}{Na}\right)_{sil} \quad (20)$$

Assuming that $[HCO_3]_{sil}$ is equivalent to $[DIC]_{sil}$, this quantity can be used in Eq. 14 to solve for $[DIC]_{DOC}$, the portion of DIC directly derived from OM respiration, either in soil pore waters, groundwaters, or during river transit. Based on this calculation, we estimate that DOC respiration can contribute up to 33% of the DIC load at some locations in the Fraser River (Table 4). Certain sites have a very low proportion of DOC respiration-derived DIC, such as the Fraser at Fitzwilliam in the Rocky Mountain headwaters (1%) and the Chilcotin River in the dry central basin (4%). The proportion of DOC respiration-derived DIC correlates strongly with DOC concentration ($r^2 = 0.53$; Fig. 6), which provides support for this approach to estimating the significance of DOC respiration.

To quantify the potential error due to the substitution of the Robson River Cl concentration described above, we performed a sensitivity analysis using Robson River Cl concentrations ranging from 2–6 µmol L^{-1}, representing the full range in observed Cl concentrations for Rocky Mountain tributaries reported in Voss et al. (2014). The chosen Cl concentration was positively correlated with the fraction of total DIC derived from OM respiration (f_{DOC}) and sites with relatively low f_{DOC} (Fraser River at Fitzwilliam, Chilcotin River) were most sensitive to the choice of Robson River Cl concentration. The site with the highest estimated f_{DOC} value (Fraser River at Stoner) ranged from 32–35% for this range of Robson River Cl concentrations. Therefore, our estimated upper bound on the contribution of DOC respiration to the DIC load (33%) has a very small error (±1.5%) due to uncertainty in the Robson River Cl concentration.

We likewise performed a sensitivity analysis to quantify the impact of the proportion of carbonate weathering due to sulfuric acid weathering (f_S) on f_{DOC}. Considering a range of f_S values from 0.01 to 0.30, the calculated values of f_{DOC} were positively correlated with the value of f_S, and the site most sensitive to the choice of f_S was that with the lowest estimated f_{DOC} (Fraser River at Fitzwilliam). The highest calculated f_{DOC} value (corresponding to the Fraser River at Stoner) ranged from 33 to 34% over this range of f_S values, thus the exact value chosen for f_S is not critically important to this estimate of OM respiration-derived DIC.

To characterize the cumulative effect of uncertainties in the measured and estimated values used in the calculation of DOC respiration-derived DIC, we performed a Monte Carlo simulation based on known or approximated uncertainties in the input parameters of

Eqs. 1–20. For parameters with analytically quantified uncertainty, we used these values for the standard deviation; for parameters with unknown uncertainty, we applied a standard deviation of 20% (Table S5). The only exception is the Robson River Cl concentration, for which we applied a standard deviation of 80% to reflect the range of potential values described above. We assumed normal distributions for all parameters and generated 10,000 simulated values for each parameter for the site with the highest calculated DOC respiration-derived DIC fraction, the Fraser River at Stoner. Based on this exercise, we estimate that the maximum f_{DOC} in the Fraser River is 0.33 ± 0.11.

The assumption that carbonate and silicate weathering, DOC respiration, and atmospheric CO_2 invasion are the sole sources of DIC is imperfect. For instance, potential DIC contributions from sulfuric acid carbonate weathering are not fully characterized by our data. Additionally, we neglected potential losses from mineral precipitation, CO_2 efflux, abiotic DOC mineralization (i.e., photo-oxidation), or in situ autotrophic uptake, and their associated stable isotope fractionations. Nevertheless, the strong correlation between DOC-respiration-derived DIC and DOC concentration clearly points to DOC as an important source of DIC in this fluvial system. We also emphasize that our estimates are based on a single sampling campaign. Given the significant seasonal variability in DOC concentrations in the Fraser River, the DIC contribution from DOC respiration likely also varies seasonally. As our study relies on samples collected along the main steam and near the outlets of major tributaries, we also cannot decipher whether the majority of DOC respiration occurs in soil porewaters, in groundwater, or in the stream and river network itself. Further study is also needed to evaluate to what extent the controls on aquatic microbial respiration are physiological (Raymond et al. 2016; Catalán et al. 2016) or biochemical (i.e., the chemical nature of DOC inhibits complete metabolism or seasonal changes in water temperature affect bacterial respiration rates).

Placing carbon cycling in the Fraser Basin within a global context

There is growing recognition that rivers do not simply serve as pipelines that transfer carbon exported from terrestrial landscapes to the ocean, but rather function as reactors where carbon is supplied, processed, and remineralized by myriad biological and physicochemical processes during transit from source to sink (Ward et al. 2017). Dissolved organic matter appears to play an important role along the aquatic continuum, both as a major mode of carbon input, but also as a key vector in the cycling of carbon between the biosphere, hydrosphere, and atmosphere. In the

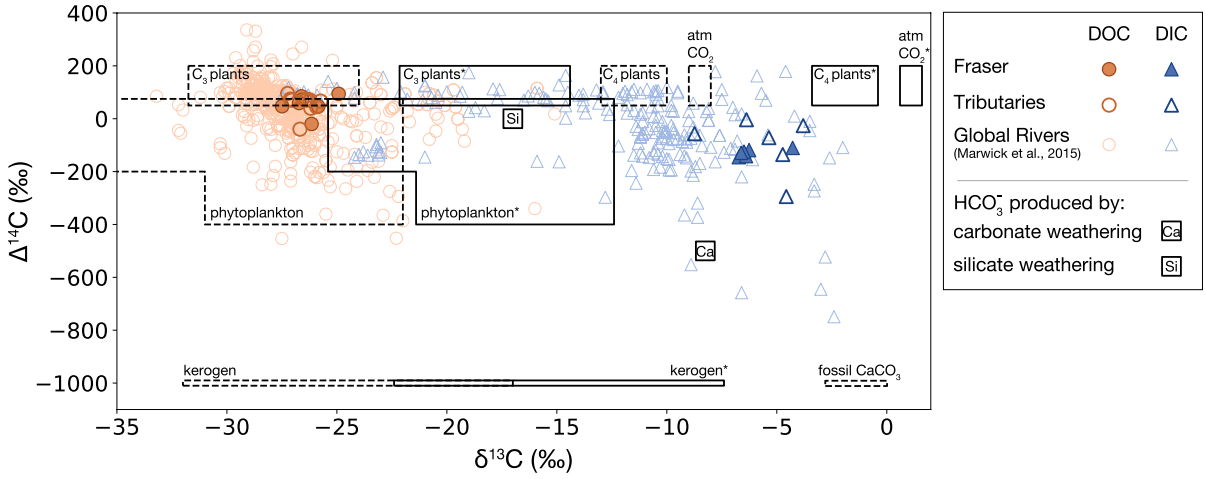

Fig. 7 Radiocarbon ($\Delta^{14}C$, ‰) and stable carbon isotope ($\delta^{13}C$, ‰) compositions of DOC and DIC in the Fraser River in the context of global river variability (after Marwick et al. 2015). Hypothetical end-members are shown both in their natural form (dashed outlines) and as "HCO_3^- equivalents" (solid outlines and * labels) accounting for a fractionation effect between $CO_2(g)$ and $HCO_3^-(aq)$ of 9.6‰, assuming a temperature of 10 °C (Clark and Fritz 1997)

Fraser Basin, we find a strong coupling between DOC and the portion of DIC that originates from DOC respiration.

The carbon isotopic signatures of Fraser River DOC and DIC are consistent with many large rivers globally (Fig. 7; Marwick et al. 2015), implying that the sources and underlying processes contributing to dissolved carbon carried by the river are representative of many major fluvial systems. In the case of DOC, the Fraser River falls well within the range of values exhibited by rivers globally for $\delta^{13}C$ composition and ^{14}C age; all of our observed Fraser River $\Delta^{14}C$-DOC values are near the center of the global distribution (median 46‰; Marwick et al. 2015), with the exception of the relatively aged samples from the Rocky Mountain region, indicating some contribution from deep soil or anthropogenic combustion-derived OM. The range of $\delta^{13}C$-DIC values in the Fraser River is on the more positive end of the full global range, and roughly in the middle between atmospheric CO_2 and carbonate weathering, with some samples trending towards the silicate weathering/organic matter end-members. The ^{14}C composition of Fraser River DIC is average compared to rivers globally, being slightly more aged than modern atmospheric CO_2.

Together, the ^{13}C and ^{14}C composition of Fraser River DIC support the interpretation of a mixture between weathering of mineral carbonate and modern sources such as atmospheric CO_2 (precipitation, gas exchange), as well as respiration of biogenic OM. The modest DOC concentrations of the Fraser River and most of its tributaries (mean of the basin-wide dataset in this study = 3 mg L^{-1}) and the generally modern $\Delta^{14}C$-DOC values we observed do not indicate significant anthropogenic disturbance of the river's DOC load. As a consequence of anthropogenic climate change, the Fraser watershed is experiencing rising temperatures (which may mobilize aged OM in mountainous areas) and more severe wildfires (which may deposit a mixture of modern vegetation-derived and aged soil-derived OM on the landscape). Future studies which characterize the impacts of these changes on the age of DOC and DIC in the Fraser River may further elucidate the sources of carbon to these pools and the magnitude of DIC production from OM mineralization.

Conclusions

The sources of DIC and DOC in the Fraser basin are spatially decoupled, yet their downstream dynamics appear to be intertwined. Carbonate weathering as a source of DIC is pronounced in certain headwater basins (Robson and McGregor rivers), as indicated by high DIC concentrations, relatively low $\Delta^{14}C$-DIC values, and high ratios of dissolved Ca/Na and Mg/Na. Downstream of these basins, tributaries carrying a disproportionately high DOC load (Blackwater, Nechako, and Willow rivers) enter the Fraser. Despite this spatial variability, DIC and DOC concentrations broadly parallel one another along the course of the Fraser main stem. Using a mass balance approach based on major ion ratios and carbon isotope compositions, we estimate that DOC respiration accounts for up to $33 \pm 11\%$ of the DIC load in some parts of the Fraser basin, while in others the DOC contribution to DIC is insignificant. The Fraser River is an ideal setting for this type of investigation on account of its wide natural variability in lithology and biogeoclimatic zones, and its limited anthropogenic disturbance. To better constrain estimates of carbon sources and fluxes, future studies would benefit from seasonal sampling and the addition of other carbon pools (particulate organic and inorganic carbon, soil carbonates, groundwater, and hot springs in the Coast Range), as well as simultaneous stable sulfur and oxygen isotope analysis of dissolved sulfate to refine the estimate of sulfuric acid weathering. Estimations of petrogenic carbon weathering fluxes, for instance based on the dissolved rhenium proxy (Hilton et al. 2014), would also help to better constrain the dissolved carbon budget of the Fraser River. Studies like this are important to assess the relative importance of mineral weathering and OC respiration in the terrestrial aquatic continuum, and to predict future carbon cycle changes in aquatic ecosystems in the face of regional and global environmental change.

Acknowledgements This work was supported by the WHOI Academic Programs Office, the MIT EAPS Department Student Assistance Fund, and the PAOC Houghton Fund to BMV, NSF-ETBC grants OCE-0851015 to BPE, VG, and TIE, and OCE-0851101 to RGMS, NSF grant EAR-1226818 to BPE, NSF grant OCE-0928582 to TIE and VG, and a WHOI Arctic Research Initiative grant to ZAW. We thank Katherine Kirsch, Sarah Rosengard, Steven Marsh, Sharon Gillies, and numerous students of the University of the Fraser Valley for assistance in the field, and the staff of

NOSAMS and the ETH-Zürich Laboratory for Ion Beam Physics for analytical support with radiocarbon measurements. We thank Hannah Gies at ETH-Zürich for preparing the figure containing data from Marwick et al. (2015). We also thank two anonymous reviewers whose thoughtful comments improved the manuscript.

Authors contribution BV, TE, BPE, and VG contributed to the study conception and design and material preparation. The first draft of the manuscript was written by BV. All authors contributed to data collection and analysis, commented on previous versions of the manuscript, and read and approved the final manuscript.

Funding Open Access funding provided by the MIT Libraries. This work was supported by the WHOI Academic Programs Office, the MIT EAPS Department Student Assistance Fund, and the PAOC Houghton Fund to BMV; NSF-ETBC grants OCE-0851015 to BPE, VG, and TIE and OCE-0851101 to RGMS; NSF grant EAR-1226818 to BPE; NSF grant OCE-0928582 to TIE and VG; and a WHOI Arctic Research Initiative grant to ZAW.

Data availability All data generated or analyzed during this study are included in this published article and its supplementary information file. Additionally, sample metadata are available in the System for Earth Sample Registration (SESAR) database at www.geosamples.org. See Table S2 for sample codes.

Declarations

Conflict of interest The authors have no relevant financial or non-financial interests to disclose.

Open Access This article is licensed under a Creative Commons Attribution 4.0 International License, which permits use, sharing, adaptation, distribution and reproduction in any medium or format, as long as you give appropriate credit to the original author(s) and the source, provide a link to the Creative Commons licence, and indicate if changes were made. The images or other third party material in this article are included in the article's Creative Commons licence, unless indicated otherwise in a credit line to the material. If material is not included in the article's Creative Commons licence and your intended use is not permitted by statutory regulation or exceeds the permitted use, you will need to obtain permission directly from the copyright holder. To view a copy of this licence, visit http://creativecommons.org/licenses/by/4.0/.

References

Aufdenkampe AK, Mayorga E, Raymond PA et al (2011) Riverine coupling of biogeochemical cycles between land, oceans, and atmosphere. Front Ecol Environ 9:53–60. https://doi.org/10.1890/100014

Battin TJ, Luyssaert S, Kaplan LA et al (2009) the boundless carbon cycle. Nature Geosci 2:598–600. https://doi.org/10.1038/ngeo618

Beaupré SR, Druffel ERM, Griffin S (2007) A low-blank photochemical extraction system for concentration and isotopic analyses of marine dissolved organic carbon: marine DOC concentration and isotope ratios. Limnol Oceanogr Methods 5:174–184. https://doi.org/10.4319/lom.2007.5.174

Blattmann TM, Wang S-L, Lupker M et al (2019) Sulphuric acid-mediated weathering on Taiwan buffers geological atmospheric carbon sinks. Sci Rep 9:2945. https://doi.org/10.1038/s41598-019-39272-5

Burke A, Present TM, Paris G et al (2018) Sulfur isotopes in rivers: insights into global weathering budgets, pyrite oxidation, and the modern sulfur cycle. Earth Planet Sci Lett 496:168–177. https://doi.org/10.1016/j.epsl.2018.05.022

Butman D, Raymond PA (2011) Significant efflux of carbon dioxide from streams and rivers in the United States. Nature Geosci 4:839–842. https://doi.org/10.1038/ngeo1294

Butman D, Stackpoole S, Stets E et al (2016) Aquatic carbon cycling in the conterminous United States and implications for terrestrial carbon accounting. Proc Natl Acad Sci USA 113:58–63. https://doi.org/10.1073/pnas.1512651112

Cai W-J (2011) Estuarine and coastal ocean carbon paradox: CO_2 sinks or sites of terrestrial carbon incineration? Annu Rev Mar Sci 3:123–145. https://doi.org/10.1146/annurev-marine-120709-142723

Calmels D, Gaillardet J, Brenot A, France-Lanord C (2007) Sustained sulfide oxidation by physical erosion processes in the Mackenzie river basin: climatic perspectives. Geology 35:1003. https://doi.org/10.1130/G24132A.1

Cameron EM (1996) Hydrogeochemistry of the Fraser river, British Columbia: seasonal variation in major and minor components. J Hydrol 182:209–225

Cameron EM, Hattori K (1997) Strontium and neodymium isotope ratios in the Fraser river: a riverine transect across the Cordilleran orogen. Chem Geol 137:243–253

Cameron EM, Hall GEM, Veizer J, Krouse HR (1995) Isotopic and elemental hydrogeochemistry of a major river system: Fraser river, British Columbia, Canada. Chem Geol 122:149–169

Catalán N, Marcé R, Kothawala DN, Tranvik LJ (2016) Organic carbon decomposition rates controlled by water retention time across inland waters. Nature Geosci 9:501–504. https://doi.org/10.1038/ngeo2720

Clark ID, Fritz P (1997) Tracing the Carbon Cycle. Environmental Isotopes in Hydrogeology. CRC Press, Boca Raton, pp 111–136

Cole JJ, Caraco NF (2001) Carbon in catchments: connecting terrestrial carbon losses with aquatic metabolism. Mar Freshwater Res 52:101–110

Cooper LW, McClelland JW, Holmes RM et al (2008) Flow-weighted values of runoff tracers $\delta^{18}O$, DOC, Ba, alkalinity) from the six largest Arctic rivers. Geophys Res Lett 35:L18606. https://doi.org/10.1029/2008GL035007

Coppola AI, Wiedemeier DB, Galy V et al (2018) Global-scale evidence for the refractory nature of riverine black carbon.

Nature Geosci 11:584–588. https://doi.org/10.1038/s41561-018-0159-8
Dickson A (2010) Standards for ocean measurements. Oceanography 23:34–47. https://doi.org/10.5670/oceanog.2010.22
Eglinton TI, Repeta DJ (2014) Organic Matter in the Contemporary Ocean. In: Holland H, Turekian K (eds) Treatise on Geochemistry. Elsevier, Amsterdam, pp 151–189
Gaillardet J, Dupré B, Louvat P, Allègre CJ (1999) Global silicate weathering and CO_2 consumption rates deduced from the chemistry of large rivers. Chem Geol 159:3–30
Galy V, Peucker-Ehrenbrink B, Eglinton T (2015) Global carbon export from the terrestrial biosphere controlled by erosion. Nature 521:204–207. https://doi.org/10.1038/nature14400
Graven HD, Guilderson TP, Keeling RF (2012) Observations of radiocarbon in CO_2 at La Jolla, California, USA 1992–2007: analysis of the long-term trend. J Geophys Res. https://doi.org/10.1029/2011JD016533
Guo L, Cai Y, Belzile C, Macdonald RW (2012) Sources and export fluxes of inorganic and organic carbon and nutrient species from the seasonally ice-covered Yukon river. Biogeochemistry 107:187–206. https://doi.org/10.1007/s10533-010-9545-z
Hallett DJ, Lepofsky DS, Mathewes RW, Lertzman KP (2003) 11,000 years of fire history and climate in the mountain hemlock rain forests of southwestern British Columbia based on sedimentary charcoal. Can J for Res 33:292–312. https://doi.org/10.1139/x02-177
Hedges JI, Keil RG, Benner R (1997) What happens to terrestrial organic matter in the ocean? Org Geochem 27:195–212. https://doi.org/10.1016/S0146-6380(97)00066-1
Hemingway JD, Spencer RGM, Podgorski DC et al (2019) Glacier meltwater and monsoon precipitation drive Upper Ganges Basin dissolved organic matter composition. Geochim Cosmochim Acta 244:216–228. https://doi.org/10.1016/j.gca.2018.10.012
Hemingway JD, Olson H, Turchyn AV et al (2020) Triple oxygen isotope insight into terrestrial pyrite oxidation. Proc Natl Acad Sci USA 117:7650–7657. https://doi.org/10.1073/pnas.1917518117
Hilton RG, West AJ (2020) Mountains, erosion and the carbon cycle. Nat Rev Earth Environ 1:284–299. https://doi.org/10.1038/s43017-020-0058-6
Hilton RG, Gaillardet J, Calmels D, Birck J-L (2014) Geological respiration of a mountain belt revealed by the trace element rhenium. Earth Planet Sci Lett 403:27–36. https://doi.org/10.1016/j.epsl.2014.06.021
Holmes RM, McClelland JW, Raymond PA et al (2008) Lability of DOC transported by Alaskan rivers to the Arctic Ocean. Geophys Res Lett 35:L03402. https://doi.org/10.1029/2007GL032837
Hood E, Fellman J, Spencer RGM et al (2009) Glaciers as a source of ancient and labile organic matter to the marine environment. Nature 462:1044–1047. https://doi.org/10.1038/nature08580
Jaffé R, Ding Y, Niggemann J et al (2013) Global charcoal mobilization from soils via dissolution and riverine transport to the oceans. Science 340:345–347. https://doi.org/10.1126/science.1231476
Lang SQ, McIntyre CP, Bernasconi SM et al (2016) Rapid ^{14}C analysis of dissolved organic carbon in non-saline waters. Radiocarbon 58:505–515. https://doi.org/10.1017/RDC.2016.17
Marwick TR, Tamooh F, Teodoru CR et al (2015) The age of river-transported carbon: a global perspective. Global Biogeochem Cycles 29:122–137. https://doi.org/10.1002/2014GB004911
McNichol AP, Schneider RJ, von Reden KF et al (2000) Ten years after—The WOCE AMS radiocarbon program. Nucl Instrum Methods Phys Res Sect B 172:479–484. https://doi.org/10.1016/S0168-583X(00)00093-8
Meybeck M (1986) Composition chimique des ruisseaux non pollués de France. Sci Géol Bull 39:3–77
Négrel P, Allègre CJ, Dupré B, Lewin E (1993) Erosion sources determined by inversion of major and trace element ratios and strontium isotopic ratios in river water: the Congo basin case. Earth Planet Sci Lett 120:59–76. https://doi.org/10.1016/0012-821X(93)90023-3
Nimptsch J, Woelfl S, Kronvang B et al (2014) Does filter type and pore size influence spectroscopic analysis of freshwater chromophoric DOM composition? Limnologica 48:57–64. https://doi.org/10.1016/j.limno.2014.06.003
Perdue EM, Beck KC, Reuter JH (1976) Organic complexes of iron and aluminium in natural waters. Nature 260:418–420
Raymond PA, Hartmann J, Lauerwald R et al (2013) Global carbon dioxide emissions from inland waters. Nature 503:355–359. https://doi.org/10.1038/nature12760
Raymond PA, Saiers JE, Sobczak WV (2016) Hydrological and biogeochemical controls on watershed dissolved organic matter transport: pulse-shunt concept. Ecology 97:5–16. https://doi.org/10.1890/14-1684.1
Reiman J, Xu Y (2018) Diel Variability of pCO_2 and CO_2 outgassing from the lower Mississippi river: implications for riverine CO_2 outgassing estimation. Water 11:43. https://doi.org/10.3390/w11010043
Roberts ML, Burton JR, Elder KL et al (2010) A High-Performance ^{14}C accelerator mass spectrometry system. Radiocarbon 52:228–235. https://doi.org/10.1017/S0033822200045252
Sarma VVSS, Kumar NA, Prasad VR et al (2011) High CO_2 emissions from the tropical Godavari estuary (India) associated with monsoon river discharges. Geophys Res Lett. https://doi.org/10.1029/2011GL046928
Schädel C, Bader MK-F, Schuur EAG et al (2016) Potential carbon emissions dominated by carbon dioxide from thawed permafrost soils. Nature Clim Change 6:950–953. https://doi.org/10.1038/nclimate3054
Song S, Wang ZA, Gonneea ME et al (2020) An important biogeochemical link between organic and inorganic carbon cycling: effects of organic alkalinity on carbonate chemistry in coastal waters influenced by intertidal salt marshes. Geochim Cosmochim Acta 275:123–139. https://doi.org/10.1016/j.gca.2020.02.013
Spence J, Telmer K (2005) The role of sulfur in chemical weathering and atmospheric CO_2 fluxes: evidence from major ions, $\delta^{13}C_{DIC}$, and $\delta^{34}S_{SO4}$ in rivers of the Canadian Cordillera. Geochim Cosmochim Acta 69:5441–5458. https://doi.org/10.1016/j.gca.2005.07.011
Spencer RGM (2022) Pers. comm. Unpublished Yukon River data comparing different filter pore sizes across a range of

DOC composition and concentration showed no statistical difference.

Stubbins A, Hood E, Raymond PA et al (2012) Anthropogenic aerosols as a source of ancient dissolved organic matter in glaciers. Nature Geosci 5:198–201. https://doi.org/10.1038/ngeo1403

Thorne R, Woo M (2011) Streamflow response to climatic variability in a complex mountainous environment: Fraser river basin. Hydrol Process, British Columbia, Canada. https://doi.org/10.1002/hyp.8225

Torres MA, West AJ, Clark KE et al (2016) The acid and alkalinity budgets of weathering in the Andes-Amazon system: insights into the erosional control of global biogeochemical cycles. Earth Planet Sci Lett 450:381–391. https://doi.org/10.1016/j.epsl.2016.06.012

Tranvik LJ, Downing JA, Cotner JB et al (2009) Lakes and reservoirs as regulators of carbon cycling and climate. Limnol Oceanogr 54:2298–2314. https://doi.org/10.4319/lo.2009.54.6_part_2.2298

Trumbore S (2000) Age of soil organic matter and soil respiration: radiocarbon constraints on belowground C dynamics. Ecol Appl 10:399–411

Valentine KWG, Sprout PN, Baker TE, Lavkulich LM (1978) The Soil Landscapes of British Columbia. Ministry of the Environment, Victoria

Voss BM, Peucker-Ehrenbrink B, Eglinton TI et al (2014) Tracing river chemistry in space and time: dissolved inorganic constituents of the Fraser river, Canada. Geochim Cosmochim Acta 124:283–308. https://doi.org/10.1016/j.gca.2013.09.006

Voss BM, Peucker-Ehrenbrink B, Eglinton TI et al (2015) Seasonal hydrology drives rapid shifts in the flux and composition of dissolved and particulate organic carbon and major and trace ions in the Fraser river, Canada. Biogeosciences 12:5597–5618. https://doi.org/10.5194/bg-12-5597-2015

Voss BM, Wickland KP, Aiken GR, Striegl RG (2017) Biological and land use controls on the isotopic composition of aquatic carbon in the upper Mississippi river basin. Global Biogeochem Cycles 31:1271–1288. https://doi.org/10.1002/2017GB005699

Wagner S, Coppola AI, Stubbins A et al (2021) Questions remain about the biolability of dissolved black carbon along the combustion continuum. Nat Commun 12:4281. https://doi.org/10.1038/s41467-021-24477-y

Wang ZA, Kroeger KD, Ganju NK et al (2016) Intertidal salt marshes as an important source of inorganic carbon to the coastal ocean. Limnol Oceanogr 61:1916–1931. https://doi.org/10.1002/lno.10347

Wang ZA, Lawson GL, Pilskaln CH, Maas AE (2017) Seasonal controls of aragonite saturation states in the Gulf of Maine. J Geophys Res Oceans 122:372–389. https://doi.org/10.1002/2016JC012373

Ward ND, Bianchi TS, Medeiros PM et al (2017) Where carbon goes when water flows: carbon cycling across the aquatic continuum. Front Mar Sci. https://doi.org/10.3389/fmars.2017.00007

Wheeler JO, Brookfield AJ, Gabrielese H, et al (1991) Terrane map of the Canadian Cordillera; Geological Survey of Canada, Map 1713A, scale 1:200,000.

Xu L, Roberts ML, Elder KL et al (2021) Radiocarbon in dissolved organic carbon by UV oxidation: procedures and blank characterization at NOSAMS. Radiocarbon 63:357–374. https://doi.org/10.1017/RDC.2020.102

Publisher's Note Springer Nature remains neutral with regard to jurisdictional claims in published maps and institutional affiliations.